

SUSY Normal Scalar Mass Hierarchy Reconciles $(g - 2)_\mu$, $b \rightarrow s\gamma$ and Relic Density

Howard Baer, Alexander Belyaev, Tadas Krupovnickas and Azar Mustafayev

*Department of Physics, Florida State University
Tallahassee, FL 32306, USA*

E-mail: baer@hep.fsu.edu, belyaev@hep.fsu.edu, tadas@hep.fsu.edu,
mazar@hep.fsu.edu

ABSTRACT: Recent experimental and theoretical determinations of $(g - 2)_\mu$, $\Omega_{CDM}h^2$ and $BF(b \rightarrow s\gamma)$ place exceedingly tight constraints on the minimal supergravity (mSUGRA) model. We advocate relaxing the generational universality of mSUGRA, so that GUT scale third generation scalar masses are greater than the (degenerate) first and second generation scalar masses (a normal scalar mass hierarchy (NMH)). The non-degeneracy allows for a reconciliation of all the above constraints, and also respects FCNC limits from $B_d - \bar{B}_d$ mixing and $b \rightarrow s\gamma$. The NMH SUGRA model leads to the prediction of relatively light first and second generation sleptons. This yields large rates for multilepton collider signatures at the CERN LHC and also possibly at the Fermilab Tevatron. The spectrum of light sleptons should be accessible to a $\sqrt{s} = 0.5 - 1$ TeV linear e^+e^- collider.

KEYWORDS: Supersymmetry Phenomenology, Hadron Colliders, Dark Matter, Supersymmetric Standard Model.

1. Introduction

The minimal supergravity model (mSUGRA) has long served as the paradigm supersymmetric model for testing the phenomenological consequences of weak scale supersymmetry[1]. The model is constructed by starting with the general supergravity Lagrangian of $N = 1$ supersymmetric gauge theories[2]. The gauge symmetry and matter content of the Standard Model are assumed, where now matter fermions comprise just one component of left chiral superfields, and the Higgs sector must be expanded by an additional doublet to cancel triangle anomalies. Supersymmetry breaking occurs within a postulated hidden sector, and can lead to weak scale soft SUSY breaking terms of mass $\tilde{m} = \Lambda^2/M_{Pl}$ if the SUSY breaking parameter $\Lambda \sim 10^{11}$ GeV. Motivated by the degeneracy solution to the SUSY flavor and CP problems[3], the simple choice of a flat Kähler metric can be made. This leads at tree level to degenerate scalar masses at some high mass scale, usually taken to be $M_{GUT} \sim 2 \times 10^{16}$ GeV. A simple choice of the gauge kinetic function leads also to gaugino mass unification. Taking the limit as $M_{Pl} \rightarrow \infty$ while keeping $m_{3/2}$ fixed leads to a globally supersymmetric renormalizable gauge theory where supersymmetry is broken by the presence of soft SUSY breaking terms (the MSSM). The weak scale parameters are related to those of the GUT scale by RG evolution, and electroweak symmetry is broken radiatively. The weak scale sparticle masses and mixings are determined by the parameters

$$m_0, m_{1/2}, A_0, \tan \beta, \text{sign}(\mu), \quad (1.1)$$

where m_0 is the common scalar mass, $m_{1/2}$ is the common gaugino mass, and A_0 is the common trilinear soft SUSY breaking term all valid at $Q = M_{GUT}$. Throughout this work, we will adopt the value $m_t = 175$ GeV.

The mSUGRA model as defined above determines the large number of MSSM parameters in terms of just a few parameters stipulated at $Q = M_{GUT}$, and therefore provides a very rich phenomenology in terms of just a few free parameters. However, the model has long been susceptible to criticism owing primarily to the assumption of universality, especially amongst scalar masses[4]. First, there is no theoretical reason for choosing a flat Kähler metric, and in general the scalar masses can be arbitrary. The arbitrary soft breaking masses in general lead to violation of constraints from FCNC processes[5], and complex soft breaking parameters can lead to CP violating phenomena at large rates[6]. It has been shown that even if universality is imposed at tree level, the universality will be broken by loop corrections[7]. We note here that there do exist symmetries which guarantee universality of soft breaking terms *within* a generation, for instance, $SO(10)$ gauge symmetry. But then the non-universality would still be manifest as a splitting amongst the generations, and with the Higgs boson soft masses.

In recent years, supersymmetric models have become increasingly constrained by a variety of measurements [8]. These include determination of the branching fraction $BF(b \rightarrow s\gamma)$ [9, 10, 11, 12, 13, 14], the muon anomalous magnetic moment $a_\mu = (g-2)_\mu/2$ [15] and the relic density of cold dark matter in the universe. The most recent development comes from the Muon $g - 2$ Collaboration, which published results on $(g - 2)_\mu$ for the negative muon along with earlier results on the positive muon. In addition, theoretical determinations of

$(g - 2)_\mu$ have been presented by Davier *et al.*[16] and Hagiwara *et al.*[17] which use recent data on $e^+e^- \rightarrow \text{hadrons}$ at low energy to determine the hadronic vacuum polarization contribution to the muon magnetic moment. Combining the latest experiment and theory numbers, we find the deviation of a_μ to be:

$$\Delta a_\mu = (27.1 \pm 9.4) \times 10^{-10} \quad (\text{Davier } et al.) \quad (1.2)$$

$$\Delta a_\mu = (31.7 \pm 9.5) \times 10^{-10} \quad (\text{Hagiwara } et al.). \quad (1.3)$$

The Davier *et al.* group also presents a number using τ decay data to determine the hadronic vacuum polarization, which gives $\Delta a_\mu = (12.4 \pm 8.3) \times 10^{-10}$, *i.e.* nearly consistent with the SM prediction. However, there seems to be growing consensus that the numbers using the e^+e^- data are more to be trusted, since they offer a direct determination of the hadronic vacuum polarization. The $\sim 3\sigma$ deviation in a_μ using the e^+e^- data can be explained in a supersymmetric context if second generation sleptons (smuons and mu sneutrinos) and charginos and neutralinos are relatively light[18].

In SUSY models with minimal flavor violation, the flavor changing decay $b \rightarrow s\gamma$ can still occur. The decay proceeds via Feynman graphs including $\tilde{t}_{1,2}\widetilde{W}_{1,2}$ and tH^+ loops, in addition to the SM contribution from a tW loop. The branching fraction $BF(b \rightarrow s\gamma)$ has recently been measured by the BELLE[9], CLEO[10] and ALEPH[11] collaborations. Combining statistical and systematic errors in quadrature, these measurements give $(3.36 \pm 0.67) \times 10^{-4}$ (BELLE), $(3.21 \pm 0.51) \times 10^{-4}$ (CLEO) and $(3.11 \pm 1.07) \times 10^{-4}$ (ALEPH). A weighted averaging of these results yields $BF(b \rightarrow s\gamma) = (3.25 \pm 0.37) \times 10^{-4}$. To this we should add uncertainty in the theoretical evaluation, which within the SM dominantly comes from the scale uncertainty, and is about 12%.¹ Experiment and theory together imply the bound,

$$BF(b \rightarrow s\gamma) = (3.25 \pm 0.54) \times 10^{-4}. \quad (1.4)$$

The calculation of SM and supersymmetric contributions to $BF(b \rightarrow s\gamma)$ used here is based upon the program of Ref. [14]. Since the SM value of $BF(b \rightarrow s\gamma)$ is relatively close to the central measured value, rather large values of $m_{\tilde{t}_{1,2}}$, $m_{\widetilde{W}_{1,2}}$ and m_{H^+} are expected, which help to suppress the SUSY loop contributions to the decay amplitude.

Finally, the recent precision mapping of anisotropies in the cosmic microwave background radiation by the WMAP collaboration have fitted the relic density of cold dark matter (CDM) in a Λ CDM universe[19, 20]. The constraint on the relic density of neutralinos produced in the early universe is then

$$\Omega_{\tilde{Z}_1} h^2 = 0.1126 \pm 0.0081. \quad (1.5)$$

The new relic density constraint is highly restrictive. In the mSUGRA model, only a few regions give rise to this narrow band of $\Omega_{\tilde{Z}_1} h^2$:

¹We caution the reader that the SUSY contribution may have a larger theoretical uncertainty, particularly if $\tan\beta$ is large. An additional theoretical uncertainty that may increase the branching ratio in the SM is pointed out in Ref. [12].

- The bulk region at low m_0 and low $m_{1/2}$, where neutralino annihilation in the early universe proceeds dominantly via t -channel slepton exchange. This region is now largely excluded (save where it overlaps with the stau co-annihilation region) because the WMAP allowed region gives rise to low values of m_h in conflict with LEP2 bounds, and also large deviations in the $BF(b \rightarrow s\gamma)$.
- The stau co-annihilation region at low m_0 where $m_{\tilde{\tau}_1} \simeq m_{\tilde{Z}_1}$, so that $\tilde{Z}_1 - \tilde{\tau}_1$ and $\tilde{\tau}_1^+ - \tilde{\tau}_1^-$ co-annihilation provides a ready sink for neutralinos in the early universe[21].
- The hyperbolic branch/focus point region (HB/FP) at large m_0 near the boundary of parameter space where μ^2 becomes small[22]. The \tilde{Z}_1 becomes increasingly higgsino-like in this region, facilitating its annihilation rate into WW , ZZ and Zh in the early universe.
- The A -resonance annihilation region at large $\tan\beta$, where $2m_{\tilde{Z}_1} \sim m_A$, m_H . In this region, the A and H widths can be quite broad ($\sim 10 - 40$ GeV), giving rise to a relatively broad A - annihilation “funnel”[23].

In addition, other regions can occur such as the h resonance annihilation region (a very narrow strip at low $m_{1/2}$ where $2m_{\tilde{Z}_1} \simeq m_h$) and stop co-annihilation region (at the edge of parameter space for very particular values of A_0 parameter).

A recent χ^2 analysis of $\Omega_{\tilde{Z}_1} h^2$, Δa_μ and $BF(b \rightarrow s\gamma)$ has been made[24], and has found the HB/FP, A -funnel and stau regions to coincide with all experimental constraints. The analysis of Ref. [24] pre-dated the new experimental and theoretical determinations of Δa_μ ². The improved Δa_μ numbers, as determined experimentally by E821 and theoretically by Davier *et al.* and by Hagiwara *et al.*, point to a larger deviation from the SM, and in particular, to relatively light second generation slepton masses, which do not occur in the HB/FP region, or in the large $m_{1/2}$ part of the A -funnel or stau co-annihilation region of the mSUGRA model.

Our goal in this paper is first to present updated χ^2 fits to the mSUGRA model, including the new Δa_μ determination. While the new Δa_μ numbers prefer lighter sleptons, the $BF(b \rightarrow s\gamma)$ numbers prefer heavy squarks, typically in the several TeV range. The tension between these two constraints, coupled with the tight $\Omega_{\tilde{Z}_1} h^2$ limits from WMAP, leave only small viable portions of mSUGRA parameter space. We present these results in Sec. 2.

In Sec. 3, we advocate relaxing the universality assumption of the mSUGRA model. In this case, constraints from FCNC processes must be addressed. The FCNC constraints apply most strongly to first and second generation scalar masses. We explore a scenario in which first and second generation scalars remain degenerate, while allowing for a significant splitting with third generation scalars. In this case, heavy (multi-TeV) third generation scalars are preferred by $BF(b \rightarrow s\gamma)$ constraints, while rather light first and second generation scalars are preferred by Δa_μ . The scenario is called the normal scalar mass hierarchy

²Explicitly, the theory calculation of Narison[25] using $e^+e^- \rightarrow hadrons$ data was used, which gave $\Delta a_\mu = (24.1 \pm 14) \times 10^{-10}$, *i.e.* just a 1.7σ deviation from the SM prediction.

(NMH), to distinguish it from earlier studies which advocated an inverted scalar mass hierarchy (IMH)[26]. The scenario respects constraints from $B_d - \bar{B}_d$ mixing. The resulting model parameter space only allows low values of $m_{1/2}$, save for a small portion of the HB/FP region. Significant regions of parameter space survive all three constraints as given above. Light first and second generation sleptons of mass just a few hundred GeV are characteristic to this scenario.

In Sec. 4, we examine consequences of the NMH scenario for collider experiments. When first and second generation sleptons become light, then chargino and neutralino decays to electrons and muons are enhanced, leading to large rates for distinctive multilepton plus jets plus \cancel{E}_T events at the CERN LHC, and possibly observable trilepton rates at the Fermilab Tevatron. At a linear e^+e^- collider operating at $\sqrt{s} = 0.5 - 1$ TeV, first and second generation sleptons should be accessible to discovery, while tau sleptons would likely be beyond reach.

We summarize our results in Sec. 5.

2. χ^2 fit of mSUGRA model

Our first objective is to calculate the χ^2 quantity formed from Δa_μ , $BF(b \rightarrow s\gamma)$ and $\Omega_{\tilde{Z}_1} h^2$, as given in Eq'ns (1.3-1.5). For $\Omega_{\tilde{Z}_1} h^2$, we only use the upper bound contribution to the χ^2 , since only the upper bound from WMAP is strictly applicable, *i.e.* there may be other forms of dark matter in the universe. In addition, we use the SM a_μ determination as given by Hagiwara *et al.*, which includes the latest fit to the hadronic vacuum polarization from $e^+e^- \rightarrow hadrons$ at low energy. We generate the mSUGRA model particle spectrum using Isajet 7.69[27], which includes two loop RGE running of all couplings and soft SUSY breaking terms, minimizes the one loop effective potential at an optimized scale choice (which accounts for leading two loop terms), and which implements the complete set of log and finite corrections to all sparticle masses³.

Once the superparticle mass spectrum and mixings are generated, we calculate the quantity $\Omega_{\tilde{Z}_1} h^2$ using the Isared program, which includes relativistic thermal averaging[29] of all relevant neutralino annihilation and co-annihilation processes as calculated exactly at tree level using the CompHEP program[30]. We evaluate Δa_μ as in Ref. [18], and the $BF(b \rightarrow s\gamma)$ as outlined in Ref. [14], which uses a tower of effective theories approach[31] and includes NLO corrections to the running of Wilson coefficients between $Q = M_W$ and $Q = m_b$ [32], and also includes the full set of NLO QCD corrections to the $b \rightarrow s\gamma$ process at the scale $Q = m_b$ [33]. In addition, in our calculations, we implement the running value of the b Yukawa coupling including MSSM threshold corrections for calculations above the scale $Q = M_W$ [34]. Our $BF(b \rightarrow s\gamma)$ results then agree well with those of Ref. [35] at both small and large $\tan \beta$.

For every point in mSUGRA model parameter space, we calculate the χ^2 quantity formed from Δa_μ , $BF(b \rightarrow s\gamma)$ and $\Omega_{\tilde{Z}_1} h^2$. For convenience, we plot in the m_0 vs. $m_{1/2}$ plane the quantity $\sqrt{\chi^2}$, which is color coded according to the legend shown in Fig. 1: *i.e.*

³Good agreement is found between Isajet and programs such as Suspect, SoftSUSY and Spheno in most of the mSUGRA model parameter space[28]

green regions have relatively low χ^2 , while red has a high χ^2 and yellow is intermediate. For variations in the two degrees of freedom (m_0 and $m_{1/2}$), $\chi^2 = 2.3$ ($\sqrt{\chi^2} = 1.52$) corresponds to a 1σ deviation from the combined measurements, $\chi^2 = 6.18$ ($\sqrt{\chi^2} = 2.49$) corresponds to a 2σ deviation and $\chi^2 = 11.83$ ($\sqrt{\chi^2} = 3.44$) corresponds to a 3σ deviation.

Our first results are shown in Fig. 1, where we plot for $A_0 = 0$, $\mu > 0$ and $\tan\beta$ values of 10, 30, 55 and 58. For $\mu < 0$, χ^2 fits are almost always worse, since Δa_μ favors $\mu > 0$. Variations in the A_0 parameter typically lead to no qualitative changes, save for those special A_0 values which drive the top squark mass to very low values. The gray regions are excluded theoretically, while the blue regions are excluded by LEP2 searches for chargino pair production. In Fig. 2, we present contour plots for $BF(b \rightarrow s\gamma)$, a_μ and Ωh^2 for the same parameters as Fig. 1; these figures complement those of Fig. 1 and explain the details of the χ^2 behavior.

In the $\tan\beta = 10$ case, it can be seen that almost all the m_0 vs. $m_{1/2}$ plane has very large χ^2 . This arises because in general an overabundance of dark matter is produced in the early universe, and the relic density $\Omega_{\tilde{Z}_1} h^2$ is beyond WMAP limits. There is a very narrow sliver of yellow at $m_{1/2} \sim 150$ GeV (just beyond the LEP2 limit) where $2m_{\tilde{Z}_1} \simeq m_h$, and neutralinos can annihilate through the narrow light Higgs resonance. In addition, there is an orange/yellow region at high m_0 at the edge of parameter space (the HB/FP region), with an intermediate value of χ^2 . In an earlier study[24], this region was found to have a low χ^2 value. In this case, however, the 3σ deviation from the SM of a_μ tends to disfavor the HB/FP region. In the HB/FP region, sleptons are so heavy (typically 3-5 TeV), that SUSY contributions to a_μ are tiny, and the prediction is that a_μ should be in near accord with the SM calculation. The remaining green region is the narrow sliver that constitutes the stau co-annihilation region, barely visible at the left hand edge of parameter space adjacent to where $\tilde{\tau}_1$ becomes the LSP. The overall situation is similar when we move to $\tan\beta = 30$: the only low χ^2 region is in the stau co-annihilation corridor.

Once we move to very large $\tan\beta$ values, as shown in the third frame, then the A -annihilation funnel becomes visible, and some large regions of moderately low χ^2 appear around m_0 , $m_{1/2} \sim 500, 600$ GeV and also at 1500, 200 GeV. While the A -annihilation funnel extends over a broad region of parameter space, the upper and lower ends of the funnel are disfavored: basically, if sparticles become too heavy (the upper end), then Δa_μ becomes too small, while if sparticles become too light (the lower end), then $BF(b \rightarrow s\gamma)$ deviates too much from its central value. The final frame shows results for $\tan\beta = 58$, close to the point where parameter space begins to collapse due to an inappropriate breakdown of electroweak symmetry. The relic density is low over much of the parameter space since $2m_{\tilde{Z}_1} \sim m_A$, so a region of relatively low χ^2 appears at modest m_0 and $m_{1/2}$ values.

Our conclusion for the mSUGRA model is that almost all of parameter space is excluded or at least disfavored by the combination of the WMAP $\Omega_{\tilde{Z}_1} h^2$ limit, the new Δa_μ value, and the $BF(b \rightarrow s\gamma)$ value. The $\Omega_{\tilde{Z}_1} h^2$ constraint only allows the several regions of parameter space mentioned in Sec. 1, while $BF(b \rightarrow s\gamma)$ favors large third generation squark masses to suppress SUSY contributions to $b \rightarrow s\gamma$ decay, and Δa_μ favors relatively light second generation slepton masses, to give a significant deviation of $(g - 2)_\mu$ from

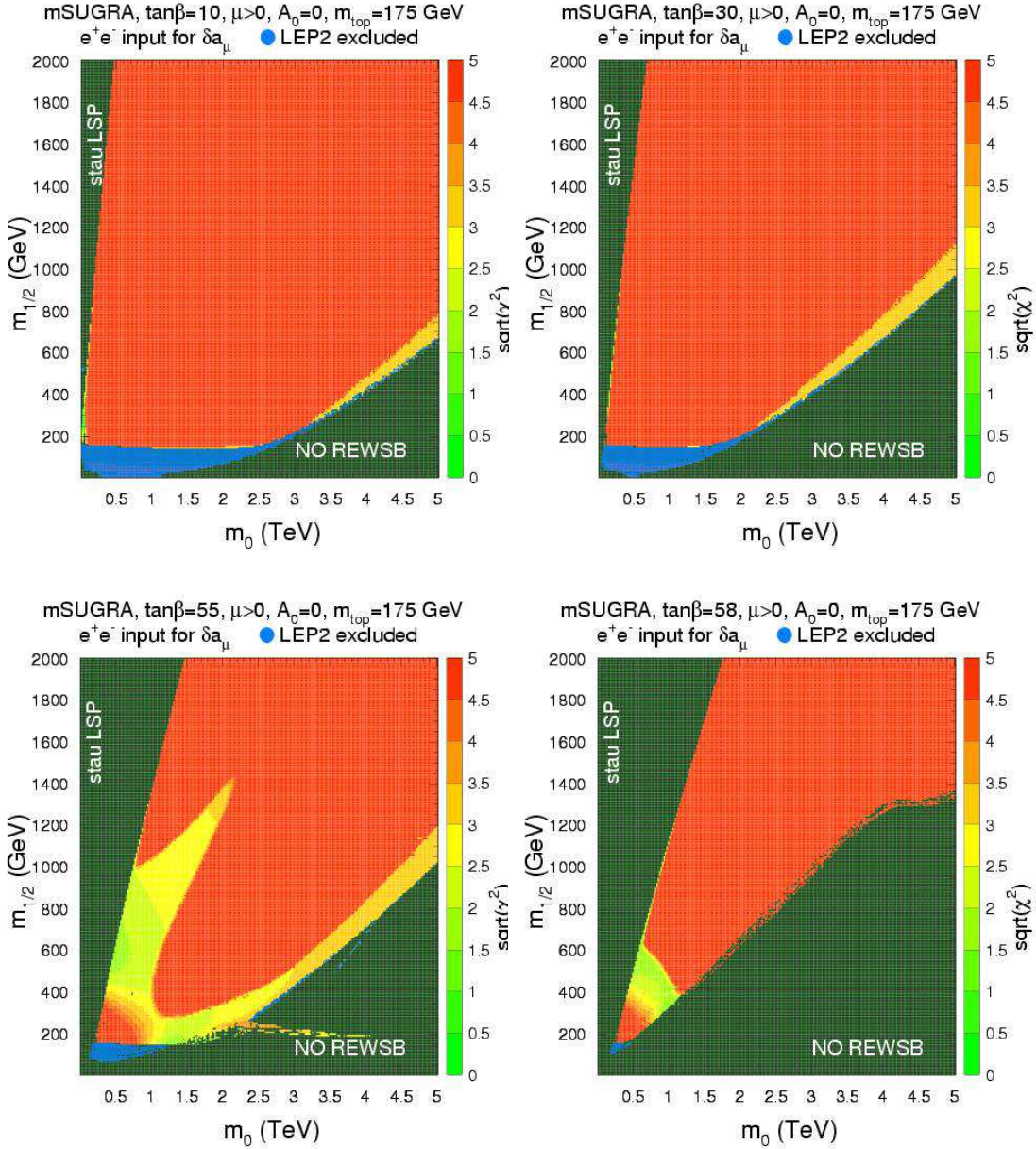


Figure 1: Plot of regions of $\sqrt{\chi^2}$ in the mSUGRA model for $A_0 = 0$, $\mu > 0$, and $\tan\beta = 10, 30, 55$ and 58 . The green regions have low χ^2 , while red regions have high χ^2 . Yellow is intermediate.

the SM value. The only surviving regions with relatively low $\sqrt{\chi^2} \lesssim 2$ are the stau co-annihilation region, and intermediate portions of the A -annihilation funnel at very large values of $\tan\beta$. The previously favored HB/FP region from Ref. [24] is now disfavored because it is unable to generate a significant deviation of $(g-2)_\mu$ from the SM prediction which uses the $e^+e^- \rightarrow \text{hadrons}$ data for evaluating the hadronic vacuum polarization graphs. (We note that should the hadronic vacuum polarization determination using τ decay data turn out to be correct, then the HB/FP region will appear in a more favorable

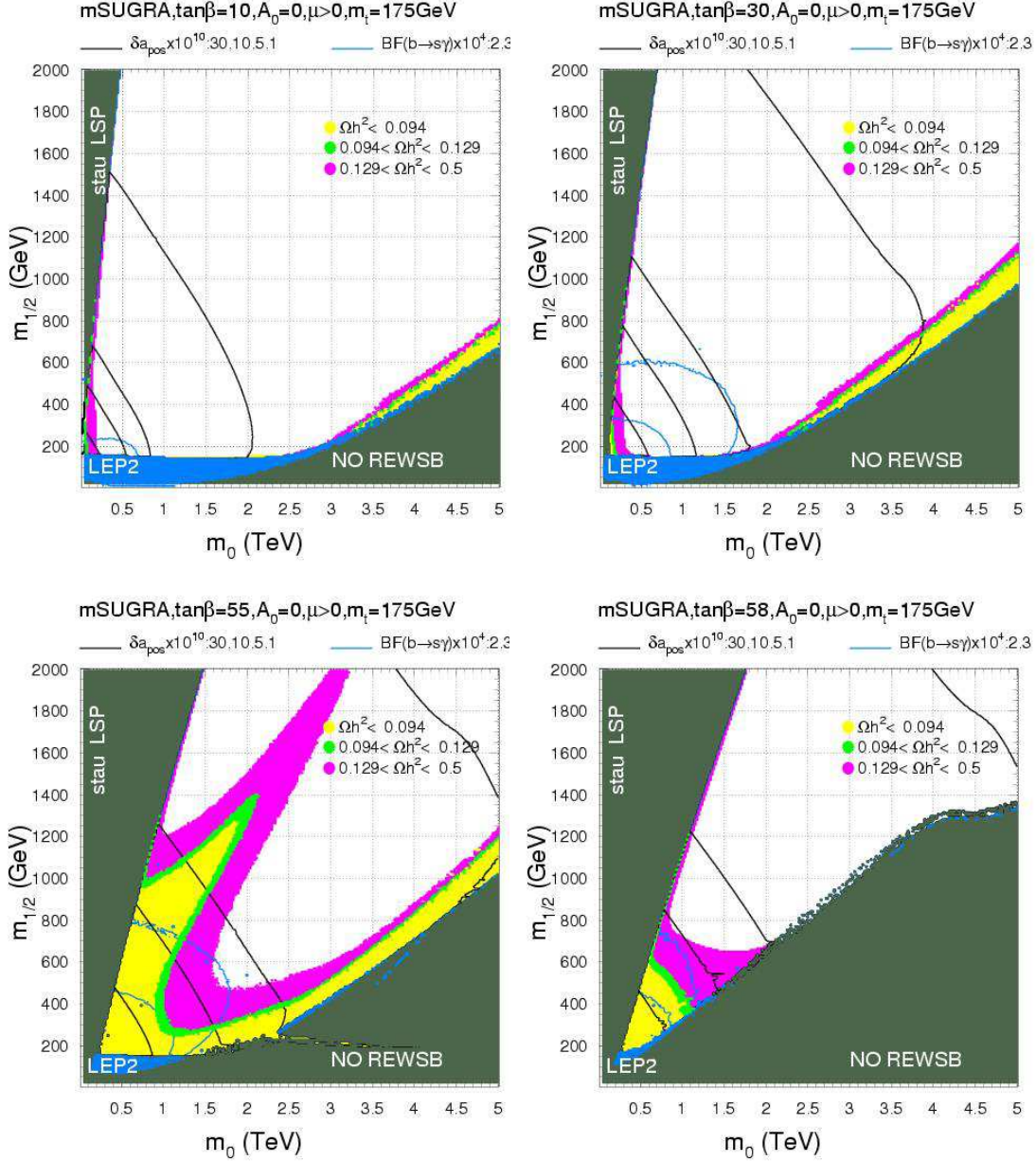


Figure 2: Contour levels for $BF(b \rightarrow s\gamma)$, a_μ and Ωh^2 in the mSUGRA model for $A_0 = 0$, $\mu > 0$, and $\tan \beta = 10, 30, 55$ and 58 . Magenta region excluded by LEP2 searches.

light!)

3. χ^2 fit of NMH SUGRA model

It is easy to see that Δa_μ favors light second generation sleptons, while $BF(b \rightarrow s\gamma)$ prefers heavy third generation squarks. This situation is hard to realize in the mSUGRA model, and may be an indication that one must move beyond the assumption of universality,

wherein each generation has a common mass at $Q = M_{GUT}$. In this section, we advocate expanding the parameter set of the mSUGRA model to the following values:

$$m_0(1), m_0(3), m_H, m_{1/2}, A_0, \tan \beta, \text{sign}(\mu). \quad (3.1)$$

In the above, $m_0(1)$ will be a common scalar mass of all *first* generation scalars at $Q = M_{GUT}$, while $m_0(3)$ is the common mass of all *third* generation scalars at M_{GUT} . m_H is the common Higgs mass at M_{GUT} . The above parameter set is well motivated in $SO(10)$ SUSY GUT models, where the two MSSM Higgs doublets typically occupy a **10** of $SO(10)$, and each generation of scalars, along with a SM gauge singlet N occupies the **16** dimensional spinorial representation of $SO(10)$. Thus, the $SO(10)$ gauge symmetry enforces universality within each generation, although each generation may be split one from another even when $SO(10)$ is unbroken. In fact, it is well known that in models where $SO(10)$ is valid beyond the GUT scale, at least the third generation of scalars will evolve to independent mass values even if all generations begin with a common mass somewhere above M_{GUT} ; see for instance, Ref. [36].

The step of breaking generational universality must be taken with some caution, since in general it can lead to violations of constraints from FCNC processes. The most stringent of the FCNC limits comes from contributions to the $K_L - K_S$ mass difference, and from limits on $\mu \rightarrow e\gamma$ decay. These bounds, however, apply to splittings between the first and second generations.

Constraints from FCNC processes are usually presented as bounds on off-diagonal terms of squark or slepton soft SUSY breaking (SSB) mass matrices or trilinear soft breaking terms in the super-CKM basis [6, 37, 38]. Here, we are interested in a “proof-of-principle” that large splittings between first and third generation scalars can exist and satisfy constraints from FCNC processes. We will assume a scenario of “minimal mixing”, where SSB mass-squared and trilinear matrices are diagonal at the electroweak scale, and that off-diagonal elements are generated *only* by rotation of the weak scale SSB matrices to the super-CKM basis⁴. In addition, in our constraint calculations we neglect the contribution of trilinear soft terms, since these contributions are often smaller than those from the mass matrices. An explicit case study is shown in the Appendix.

Within the minimal mixing scenario, the limits from the $K_L - K_S = \Delta m_K$ mass difference in the super-CKM basis can be translated to limits on mass splittings of diagonal soft SUSY breaking mass terms. In the case of equal squark and gluino masses, these bounds are roughly [38]

$$|m_{\bar{q}}(1) - m_{\bar{q}}(2)| \lesssim 2m_c \frac{m_{\bar{q}}^2}{M_W^2}, \quad (3.2)$$

which yields mass splittings for weak scale SSB squark masses of order the charm quark mass (m_c) if the average squark mass is $m_{\bar{q}} \simeq M_W$. If squark masses are much heavier, the limits become less stringent. Allowed regions of the $m_{\bar{q}}(1)$ *vs.* $m_{\bar{q}}(2)$ plane are shown in Fig. 3 for several different gluino masses. The limits are obtained from the complete gluino-squark box diagram computation, where it is conservatively required that

⁴Arbitrarily large off-diagonal SSB elements would lead to fatal conflicts with FCNC bounds.

$|\Delta m_K^{SUSY}| \leq \Delta m_K^{exp}$, and Δm_K^{exp} is the measured $K_L - K_S$ mass difference. The limits are presented assuming *i.*) just a contribution from left squark-left squark mass terms (LL: green-shaded region), or more stringently *ii.*) from the presence of both left-left and right-right (RR) squark mass terms (blue-shaded region). The less stringent constraint assumes that there is splitting only between soft SUSY breaking masses for left squarks of the 1st and 2nd generations, while the corresponding right squarks remain degenerate. In this way, non-degeneracy of up to 50% can be allowed for squarks in the TeV range. It can be seen from Fig. 3 that a liberal allowance of non-degeneracy does not work with either scenario if squarks ~ 100 GeV, because both areas converge to a line of nearly perfect degeneracy, which was the main motivation for the mSUGRA model. In this paper, in order to accommodate the kaon mass difference constraint, we will, without further discussion, maintain universality, but just between the first and second generations: $m_0(1) \simeq m_0(2)$.

Splitting the third generation from the first and second can also potentially lead to violations of FCNC processes. One of the main experimentally measured bounds on FCNC processes in this case comes from $B_H^0 - B_L^0$ mass splitting. As in the kaon case, we neglect all but the largest contribution to Δm_B coming from gluino-squark box diagrams. In this case, for equal gluino and squark masses, the soft term mass splitting limit is

$$|m_{\bar{q}}(1) - m_{\bar{q}}(3)| \lesssim \frac{m_{\bar{q}}^2}{M_W}, \quad (3.3)$$

which is much less restrictive than the kaon case, for both low and high squark masses. We adopt the result for gluino box diagrams from Ref. [37] to calculate the SUSY contribution to Δm_{B_d} . The result for various values of $m_{\bar{g}}$ is presented in the $m_{\bar{q}}(1)$ vs. $m_{\bar{q}}(3)$ plane in Fig. 4, where $m_{\bar{q}}(i)$ is the weak scale squark mass for generation i . The magenta regions give values of $|\Delta m_B^{SUSY}| < \Delta m_B^{exp}/1000$, while green gives $|\Delta m_B^{SUSY}| < \Delta m_B^{exp}/100$, and yellow gives $|\Delta m_B^{SUSY}| < \Delta m_B^{exp}/10$. From the figure, it is clear that practically the whole parameter space of NMH SUGRA model is allowed by the Δm_{B_d} constraint.

We have also checked the potential constraint on $m_0(2) - m_0(3)$ splitting from $BF(b \rightarrow s\gamma)$ measurements. These constraints also yield weak bounds on generational splitting; see the Appendix for an explicit calculation. More details can be found, for example, in Ref. [38] (see Eqs. (53-54)) and Ref. [5] (see Eq. (19)), along with discussion of these bounds.

Independent of which precise limit on Δm_B we choose, it is easy to see from Fig. 4 that any constraint on degeneracy of weak scale squark masses applies only if squark masses are quite light, well below the TeV scale. As we move to TeV level squark (and gluino) masses and beyond, the limits become essentially non-existent. This corresponds to a partial decoupling solution to the SUSY flavor problem.

However, even if squark mass splittings are very large at the scale $Q = M_{GUT}$, the weak scale mass splittings are often much smaller. As an example, we illustrate the running of soft SUSY breaking parameters in Fig. 5, where we choose

$$\begin{aligned} m_0(1) &= 100 \text{ GeV}, & m_0(3) &= m_H = 1400 \text{ GeV}, & m_{1/2} &= 550 \text{ GeV}, \\ A_0 &= 0, & \tan \beta &= 30, & \mu &> 0, & m_t &= 175 \text{ GeV}. \end{aligned} \quad (3.4)$$

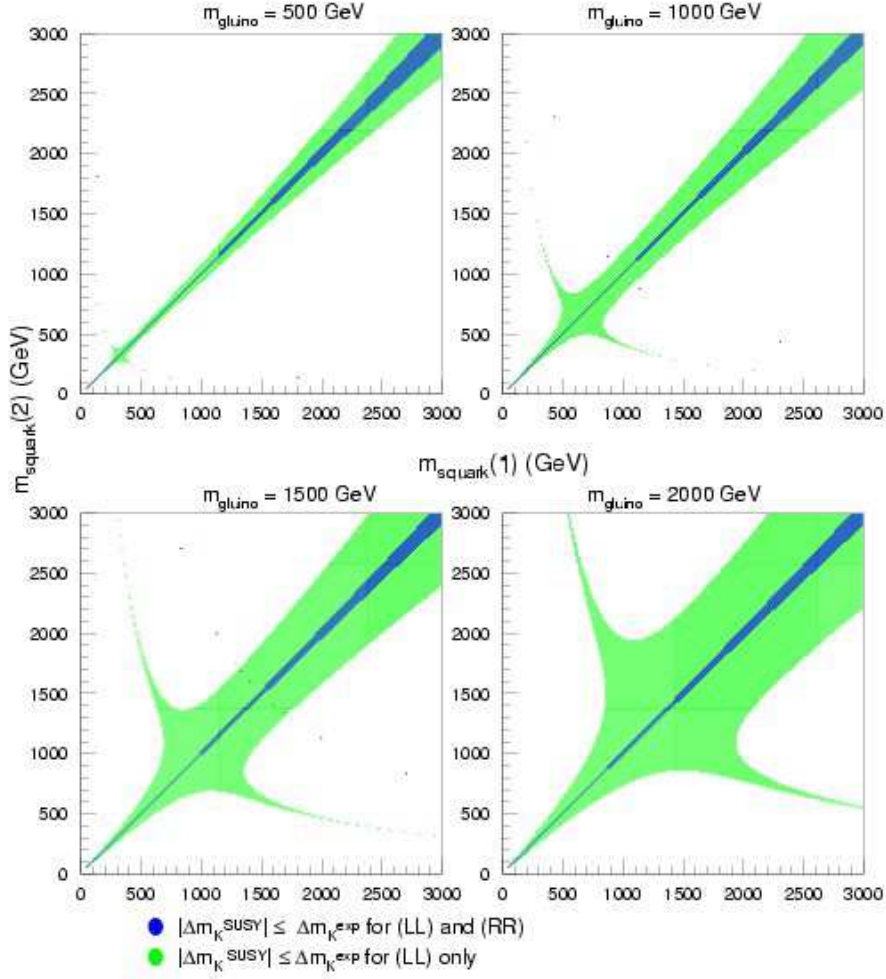


Figure 3: Constraints on first and second generation squark masses from Δm_K .

While first generation slepton masses are renormalized to values of $m_{\tilde{\ell}} \sim 100 - 300$ GeV, the first generation squark masses evolve to weak scale values in the TeV range, since the QCD contributions to RG running are large⁵. Meanwhile, the running of third generation squarks is actually suppressed somewhat, owing to the large top quark Yukawa coupling. The result is that, even beginning with a large splitting in generations at $Q = M_{GUT}$, a much less severe splitting amongst squarks may be obtained at the weak scale. Of course,

⁵A simple approximate formula relating weak scale to GUT scale squark and slepton masses is that $m_q^2 \simeq m_0^2 + (5 - 6)m_{1/2}^2$, while $m_{\tilde{\ell}}^2 \simeq m_0^2 + (0.15 - 0.5)m_{1/2}^2$.

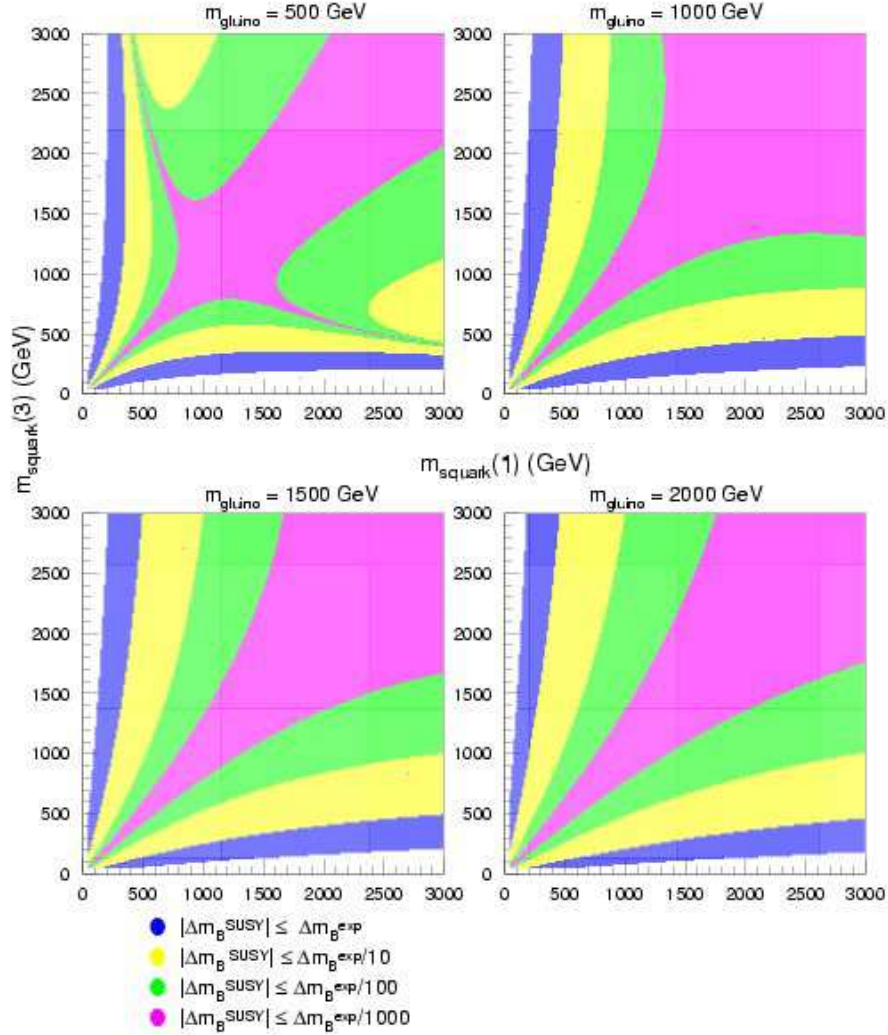


Figure 4: Constraints on first and third generation squark masses from Δm_{B_d} .

the splitting amongst sleptons remains rather large, and could give large contributions to $\tau \rightarrow e\gamma$ and $\tau \rightarrow \mu\gamma$ decay. However, the current experimental limits from flavor changing radiative τ decay are not overly constraining[6].

Motivated by above considerations, we next generate random points in the parameter space given in Eq. 3.1, and again calculate the resultant χ^2 values. We have scanned over the following region of parameter space for $sign(\mu) > 0$:

$$m_0(1) : 0 - 3 \text{ TeV}, \quad m_0(3) : 0 - 3 \text{ TeV}, \quad m_H : 0 - 3 \text{ TeV},$$

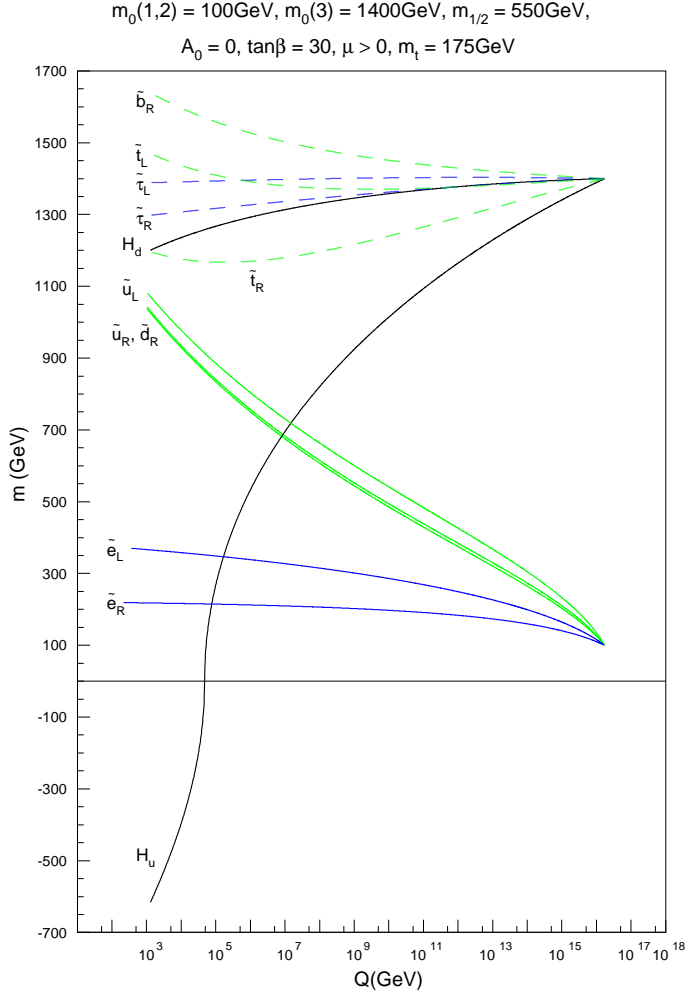


Figure 5: Evolution of soft SUSY breaking masses in the NMH SUGRA model.

$$m_{1/2} : 0 - 1 \text{ TeV}, A_0 : -3 - 3 \text{ TeV}, \tan\beta : 2 - 60. \quad (3.5)$$

The colors of the points correspond to those of Fig. 1, so that green gives low χ^2 , red gives high χ^2 , and yellow gives intermediate values. A variety of frames showing correlations amongst the parameters are shown in Fig. 6. Only points satisfying the LEP2 constraints have been plotted. This is why, for example, $m_{1/2}$ is bounded from below at $\sim 200\text{GeV}$, corresponding to the limit on the chargino mass of $m_{\tilde{W}_1} > 103.5 \text{ GeV}$.

From the top row of figures, we see that rather low values of $m_0(1) \sim 0 - 400 \text{ GeV}$ are preferred. These parameter values give sufficiently light smuon and mu sneutrino masses so as to fulfill the $(g - 2)_\mu$ constraint. Values of $m_{1/2} \sim 400 - 800 \text{ GeV}$ are preferred, although little preference is shown for A_0 . One can also see little preference for $\tan\beta$ so long as $m_0(1)$ remains small. For larger values of $m_0(1)$, there is a preference for very high values of $\tan\beta \sim 50 - 60$, as in the mSUGRA model case.

The plots of the second row show that there is some preference for $m_H \sim m_0(3)$, and that there is a preference for $m_0(1) \ll m_0(3)$. The third row shows that while $m_0(1) \sim 0-400$ GeV, $m_0(3) \sim 500-3000$ GeV is preferred. Further, the last frame of this row shows that while low χ^2 points can occur at any $\tan\beta$ value if there is a large $m_0(1) - m_0(3)$ mass splitting, that mainly large $\tan\beta$ is preferred if the generational mass splitting is small (which takes us back towards the mSUGRA case). It may also be pointed out that SUSY IMH models are greatly disfavored. Finally, the last row of plots shows the mechanism for annihilating neutralinos in the early universe. The first frame shows a region of low χ^2 where $2m_{\tilde{Z}_1} \simeq m_A$, *i.e.* the A -funnel at large $\tan\beta$, which occurs in the subset of mSUGRA like models. The second frame shows that some models get rid of neutralinos by stau co-annihilation, while the third frame shows that now many models may also destroy neutralinos in the early universe via $\tilde{Z}_1 - \tilde{e}$ and $\tilde{Z}_1 - \tilde{\mu}$ co-annihilation.

Motivated by the above scan, we next adopt the value $m_H = m_0(3)$ (to reduce parameter freedom), and plot the $\sqrt{\chi^2}$ values in the $m_0(3)$ *vs.* $m_{1/2}$ plane in Fig. 7, for $m_0(1)$ values of 50, 100 and 200 GeV, with $\tan\beta = 10$, $A_0 = 0$ and $\mu > 0$. The corresponding contour plots of $BF(b \rightarrow s\gamma)$, a_μ and Ωh^2 are shown in Fig. 8.

The most striking feature of the plots is that most of the area displayed is excluded. In this case, slepton masses are quite light, in the vicinity of a few hundred GeV. As $m_{1/2}$ increases, ultimately $m_{\tilde{Z}_1}$ becomes greater than $m_{\tilde{e}}$, and one violates the cosmological constraint on stable charged relics from the Big Bang. Of the surviving parameter space, we find significant regions with relatively low χ^2 . The plot with $m_0(1) = 50$ GeV has a rather broad band of low χ^2 . In this case, neutralinos in the early universe can annihilate by a combination of t -channel slepton exchange (as in the bulk region of mSUGRA), and by neutralino-slepton co-annihilation. In addition, smuons and mu sneutrinos are relatively light, giving a large, positive contribution to Δa_μ , while top squarks inhabit the TeV and beyond range, effectively suppressing anomalous contributions to $BF(b \rightarrow s\gamma)$. In addition to the region with low values of $m_0(3)$ and low $m_{1/2}$, a thin strip of the HB/FP region survives, where the small value of μ that is generated leads to a Higgsino-like LSP. In this case, the HB/FP has moderate but not low χ^2 values because the contribution to Δa_μ is low. Finally, we note in this plot that the stau co-annihilation region is somewhat enhanced as well on the left most boundary of parameter space. This is because neutralinos can annihilate via a combination of t -channel slepton exchange, and also stau co-annihilation.

If we shift to the $m_0(1) = 100$ GeV plot, then slepton masses correspondingly increase, suppressing the relic density in the low $m_{1/2}$ region of the plot. One must move close to the slepton co-annihilation region at the upper boundary of parameter space in order to generate a sufficiently low value of $\Omega_{\tilde{Z}_1} h^2$ in accord with the WMAP analysis. Large $m_0(3)$ values are favored over small ones only because small $m_0(3)$ implies larger $m_{1/2}$ values to get the relic density right, but then the large $m_{1/2}$ value drives up the smuon masses and thus suppresses Δa_μ too much. The further shift to $m_0(1) = 200$ GeV leads to a plot in which very little area contains a low value of χ^2 . This is due to the fact that slepton masses have increased, and neutralino annihilations graphs with t -channel slepton exchange are suppressed. Only the border region survives, where $\tilde{\mu} - \tilde{Z}_1$ and $\tilde{e} - \tilde{Z}_1$ co-annihilation occurs at a large rate.

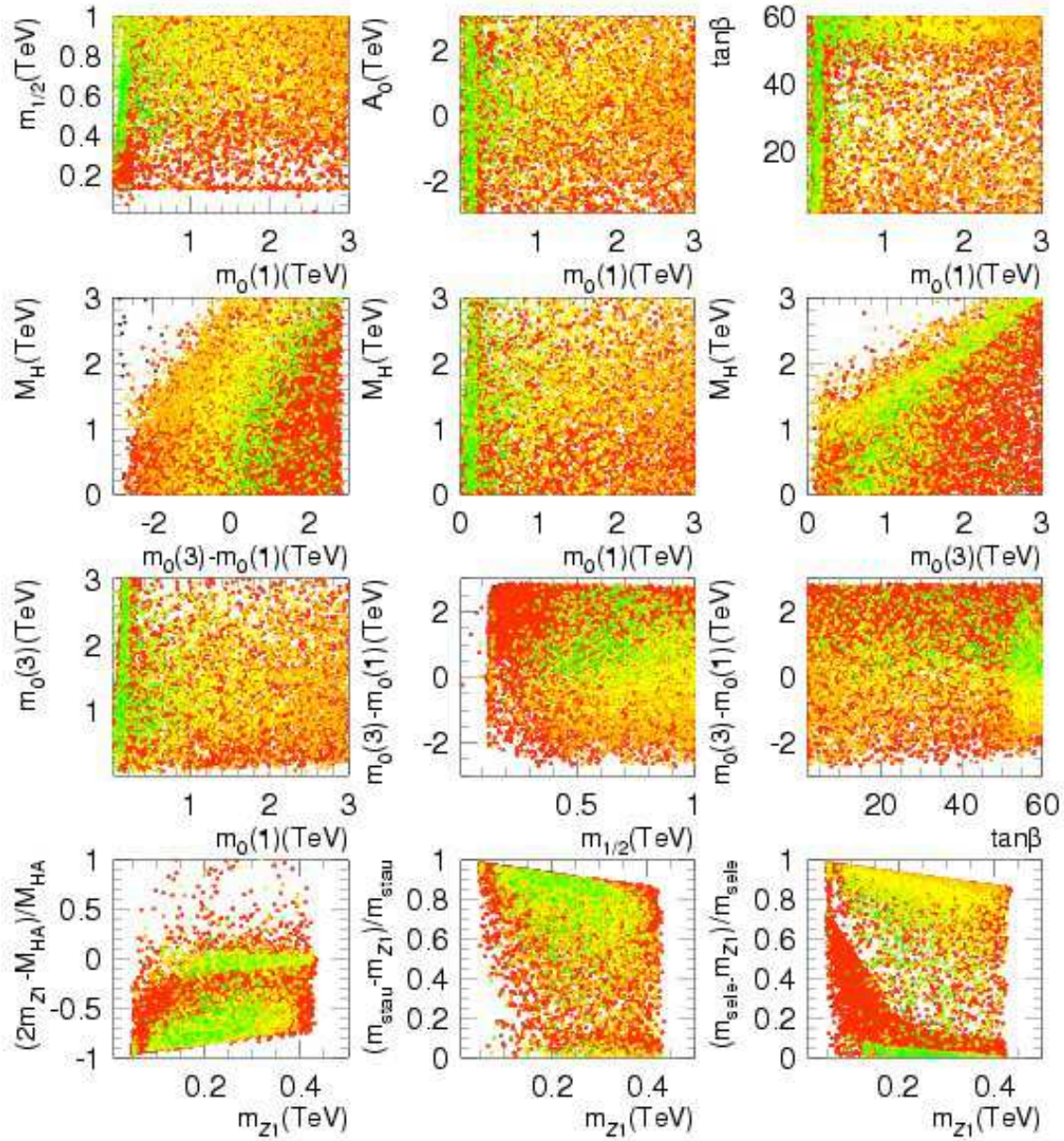


Figure 6: Scan over parameter space of NMH SUGRA model. Green points have low χ^2 , while red points have high χ^2 ; yellow points have intermediate χ^2 .

In Fig. 9, we again show the $m_0(3)$ vs. $m_{1/2}$ plane, this time for $\tan\beta = 30$, and for $m_0(1)$ values of 50, 100 and 200 GeV. Fig. 10 presents the associated $BF(b \rightarrow s\gamma)$, a_μ and Ωh^2 contour plots for the same $\tan\beta$ value.

By increasing $\tan\beta$, we also increase the SUSY contribution to a_μ for a given set of slepton and chargino/neutralino masses. The result is a band of very low χ^2 points in the $m_0(1) = 50$ and 100 GeV plots, where essentially a perfect fit to $(g - 2)_\mu$, $BF(b \rightarrow s\gamma)$

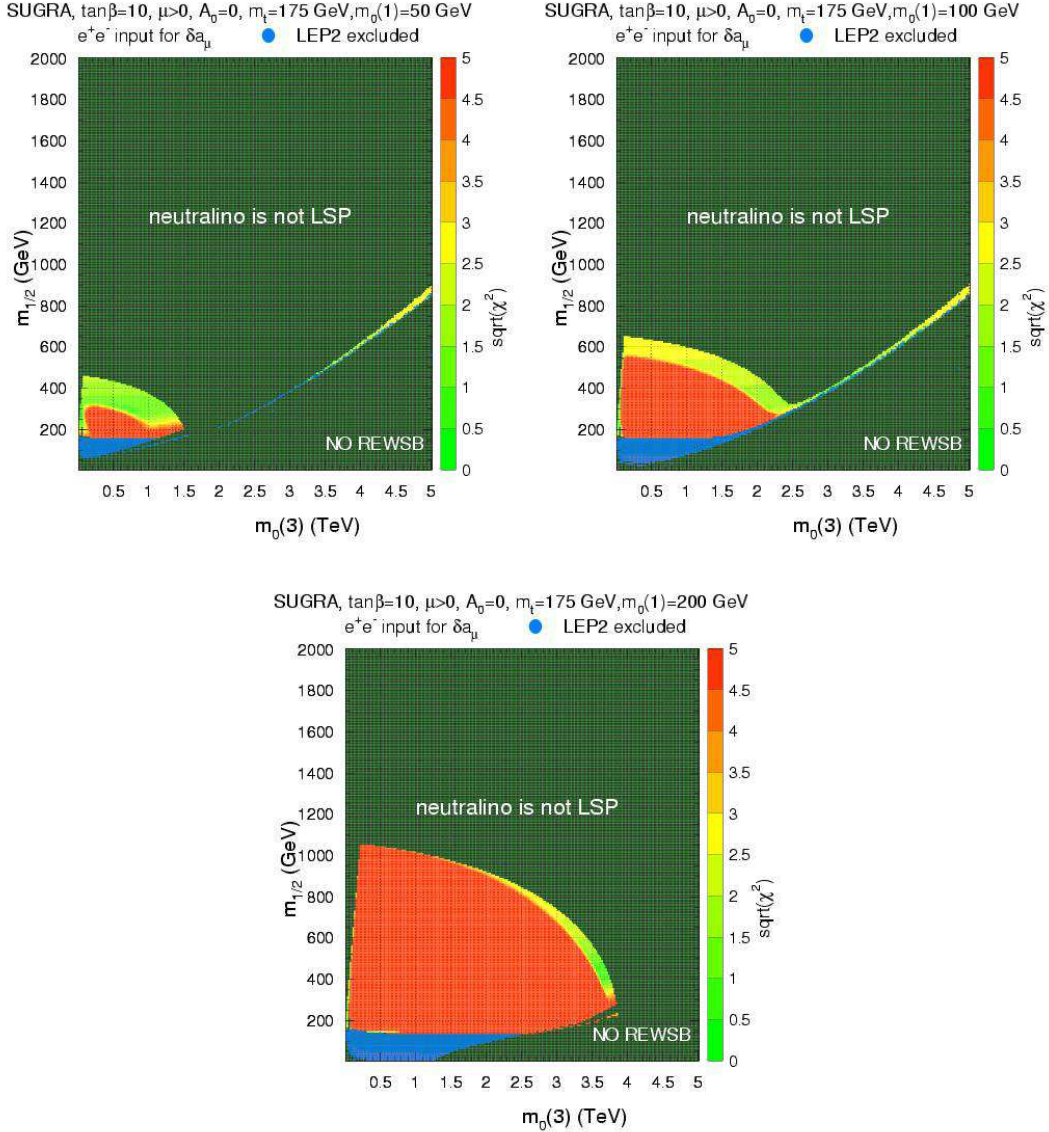


Figure 7: Plot of regions of $\sqrt{\chi^2}$ in the $m_0(3)$ vs $m_{1/2}$ plane of the NMH SUGRA model for $m_0(1,2) = 50, 100$ and 200 GeV with $A_0 = 0$, $\mu > 0$, and $\tan\beta = 10$. The green regions have low χ^2 , while red regions have high χ^2 . Yellow is intermediate.

and $\Omega_{\tilde{Z}_1} h^2$ can be obtained. The low $m_{1/2}$ portion of the $m_0(3)$ vs $m_{1/2}$ plane are largely excluded because they give rise to too large a relic density of $0.129 < \Omega_{\tilde{Z}_1} h^2 < 0.5$, and because they give rise to too large a value of Δa_μ . In these plots, we also note that the HB/FP strip has moved to a somewhat lower χ^2 value compared to the $\tan\beta = 10$ plots due to a larger SUSY contribution to Δa_μ . Sample spectrum for a point with very low χ^2 is shown in Table 1. The last frame, with $m_0(1) = 200$ GeV, has become again largely excluded, save for a narrow strip where slepton co-annihilation occurs, and in the HB/FP region.

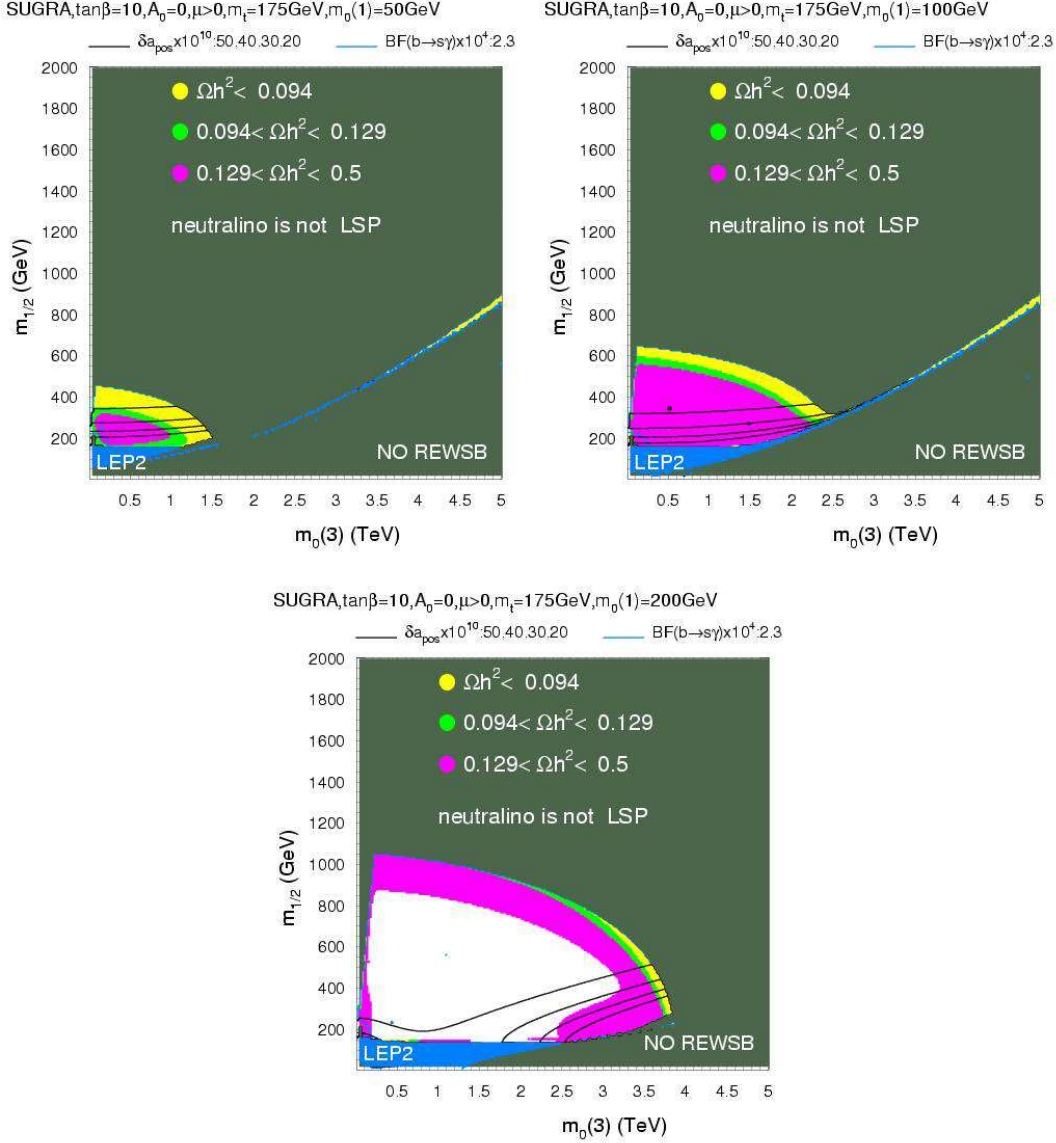


Figure 8: Contour levels for $BF(b \rightarrow s\gamma)$, a_μ and $\Omega_{\tilde{Z}_1} h^2$ in the mSUGRA model in the $m_0(3)$ vs. $m_{1/2}$ plane of the NMH SUGRA model for $m_0(1, 2) = 50, 100$ and 200 GeV with $A_0 = 0$, $\mu > 0$, and $\tan\beta = 10$. Magenta region excluded by LEP2 searches.

4. Implications for colliders

In the previous section, we have seen that the adoption of non-universal scalar masses can lead to a reconciliation of the SUSY explanation for a_μ , $BF(b \rightarrow s\gamma)$ and $\Omega_{\tilde{Z}_1} h^2$. The scenario of NMH SUGRA model works if $m_0(1) \simeq m_0(2) \ll m_0(3)$, and leads to spectra typically with squarks and third generation sleptons in the TeV range, while first and second generation sleptons have masses in the range of 100-300 GeV. The presence of rather light first and second generation sleptons in the sparticle mass spectrum in general leads to enhancements in leptonic cross sections from superparticle production at collider

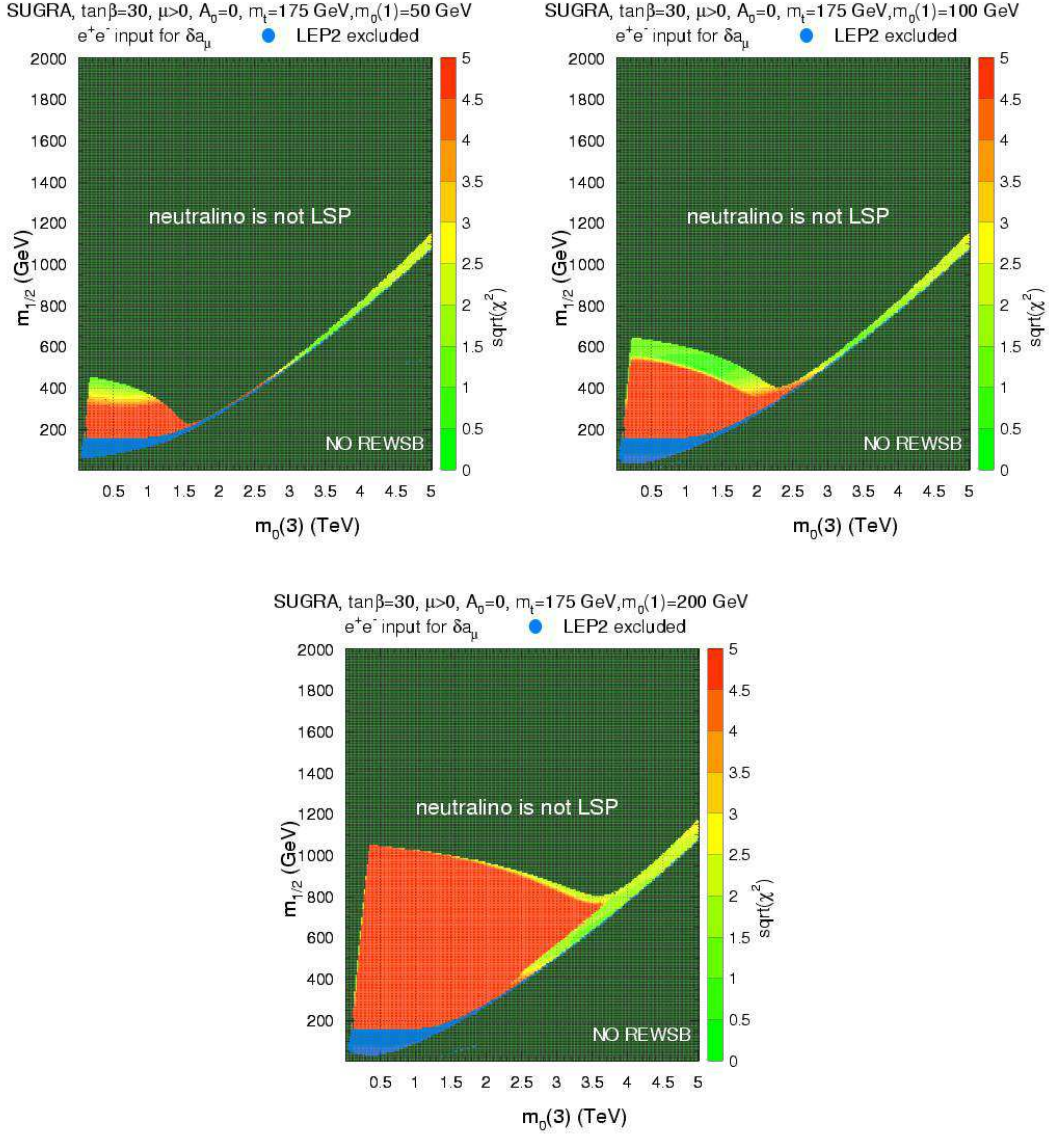


Figure 9: Plot of regions of $\sqrt{\chi^2}$ in the $m_0(3)$ vs. $m_{1/2}$ plane of the NMH SUGRA model for $m_0(1,2) = 50, 100$ and 200 GeV, with $A_0 = 0$, $\mu > 0$, and $\tan\beta = 30$. The green regions have low χ^2 , while red regions have high χ^2 . Yellow is intermediate.

experiments, compared to the case where selectrons and smuons are in the multi-TeV range. The enhancement comes from the fact that sleptons may now be produced with non-negligible cross sections at colliders, and also in that their presence enhances the leptonic branching fractions of charginos and especially neutralinos. In this section, we discuss the implications of light selectrons and smuons for the Fermilab Tevatron collider, the CERN LHC and a linear e^+e^- collider operating with $\sqrt{s} \sim 0.5 - 1$ TeV.

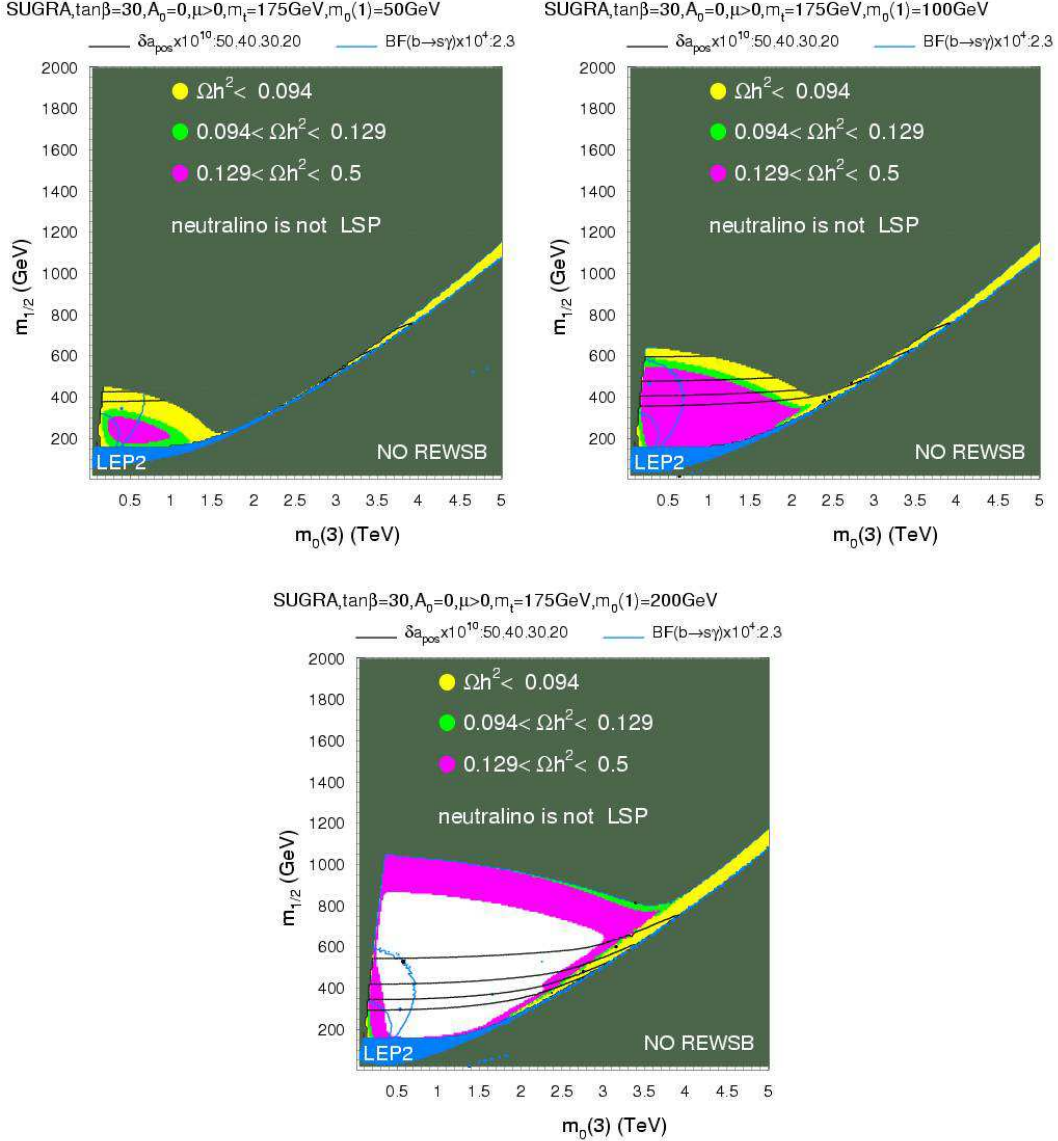


Figure 10: Contour levels for $BF(b \rightarrow s\gamma)$, a_μ and Ωh^2 in the mSUGRA model in the $m_0(3)$ vs. $m_{1/2}$ plane of the NMH SUGRA model for $m_0(1,2) = 50$ GeV, and $m_0(1,2) = 100$ GeV with $A_0 = 0$, $\mu > 0$, and $\tan\beta = 30$. Magenta region excluded by LEP2 searches.

4.1 Tevatron signals

At the Fermilab Tevatron collider, the total production cross section for slepton pair production is rather low (~ 10 fb for $m_{\tilde{\ell}} \sim 100$ GeV)[39], so that prospects for their direct detection are not encouraging[40] even with optimistic projections for the integrated luminosity to be gathered. Even so, if sleptons are light enough, then charginos and neutralinos may directly decay into them via two body modes: $\tilde{W}_1 \rightarrow \nu_{\ell} \tilde{\ell}_L$, $\tilde{\nu}_{\ell} \ell$ and $\tilde{Z}_2 \rightarrow \tilde{\ell}_R \ell$, $\tilde{\nu}_{\ell} \nu_{\ell}$ and $\tilde{\ell}_L \ell$ (we suppress bars on anti-particles). Even if two-body decays are not kinematically open, then relatively light sleptons can yield enhancements in chargino and especially

neutralino three body decay to leptons.

If sparticles are accessible to the Fermilab Tevatron, then it is usually expected that $p\bar{p} \rightarrow \widetilde{W}_1^+ \widetilde{W}_1^- X$ and $\widetilde{W}_1 \widetilde{Z}_2 X$ will be the dominant production cross sections^[41]. If $\widetilde{W}_1 \rightarrow \ell \nu_\ell \widetilde{Z}_1$ and $\widetilde{Z}_2 \rightarrow \ell \bar{\ell} \widetilde{Z}_1$, then clean trilepton signals may occur at an observable rate^[42]. Signal and background rates have recently been investigated in Ref. [43], where Tevatron reach plots may also be found. Here, we generate all sparticle production processes using Isajet 7.69 for the parameter space point $m_0(3) = 1400$ GeV, $m_{1/2} = 225$ GeV, $A_0 = 0$, $\tan\beta = 10$ and $\mu > 0$. We plot the isolated trilepton signal after using cuts SC2 of Ref. [44], where the backgrounds are also evaluated. The results, plotted versus variation in the $m_0(1)$ parameter, are shown in Fig. 11, where the signal level needed for a 5σ signal with 10 fb^{-1} is also denoted. The error bars show the Monte Carlo statistical error. When $m_0(1) = m_0(3)$ (at $m_0(1) = 1400$ GeV), the results correspond to the mSUGRA model, and the isolated trilepton signal is well below discovery threshold. As $m_0(1)$ decreases to smaller values, the isolated trilepton rate drops. This is due in part to a slight reduction in total SUSY cross section (shown in frame *b*), but also due to an interference in the \widetilde{Z}_2 leptonic decay rates, due to destructive interference between slepton and Z boson mediated graphs. As $m_0(1)$ drops to even lower values, the light sleptons begin to dominate neutralino three body decays rates, and consequently the trilepton cross section rises steeply, to the level of observability. Eventually chargino and neutralino two body decays to sleptons turn on (in this case, first $\widetilde{Z}_2 \rightarrow \tilde{\ell}_R \ell$), and trilepton rates become very high. For even lower $m_0(1)$ values, neutralino decays to $\tilde{\nu}_\ell \nu_\ell$ turn on, and briefly suppress the trilepton rate, until finally $\widetilde{Z}_2 \rightarrow \tilde{\ell}_L \ell$ turns on, and the trilepton rate picks up again for the lowest $m_0(1)$ values.

The large rates for clean trileptons at the Fermilab Tevatron occur for $m_0(1)$ values below about 200 GeV, which is just the regime needed to give substantial SUSY contributions to $(g-2)_\mu$. In the plot shown, the $m_{1/2}$ value chosen was small enough that sparticle total production cross sections are large enough to generate an observable signal. For larger $m_{1/2}$ values, an observable signal at the Fermilab

parameter	value (GeV)
M_2	351.1
M_1	184.2
μ	516.9
$m_{\tilde{g}}$	1067.7
$m_{\tilde{u}_L}$	939.8
$m_{\tilde{u}_R}$	910.0
$m_{\tilde{d}_L}$	943.5
$m_{\tilde{d}_R}$	907.1
$m_{\tilde{t}_1}$	1175.1
$m_{\tilde{t}_2}$	1477.5
$m_{\tilde{b}_1}$	1460.0
$m_{\tilde{b}_2}$	1637.1
$m_{\tilde{e}_L}$	319.3
$m_{\tilde{e}_R}$	188.2
$m_{\tilde{\nu}_e}$	295.1
$m_{\tilde{\tau}_1}$	1386.1
$m_{\tilde{\tau}_2}$	1475.4
$m_{\tilde{\nu}_\tau}$	1468.5
$m_{\widetilde{W}_1}$	348.2
$m_{\widetilde{W}_2}$	542.4
$m_{\widetilde{Z}_1}$	179.4
$m_{\widetilde{Z}_2}$	347.2
m_A	1379.3
m_h	118.4
$\Omega_{\widetilde{Z}_1} h^2$	0.115
$BF(b \rightarrow s\gamma)$	3.52×10^{-4}
Δa_μ	35.1×10^{-10}

Table 1: Masses and parameters in GeV units for $m_0(3)$, $m_{1/2}$, A_0 , $\tan\beta$, $sign(\mu) = 1500$ GeV, 450 GeV, 0, 30, +1 in the NMH SUGRA model. We also take $m_H = m_0(3)$ and $m_0(1) = 100$ GeV. The spectrum is obtained using ISAJET v7.69.

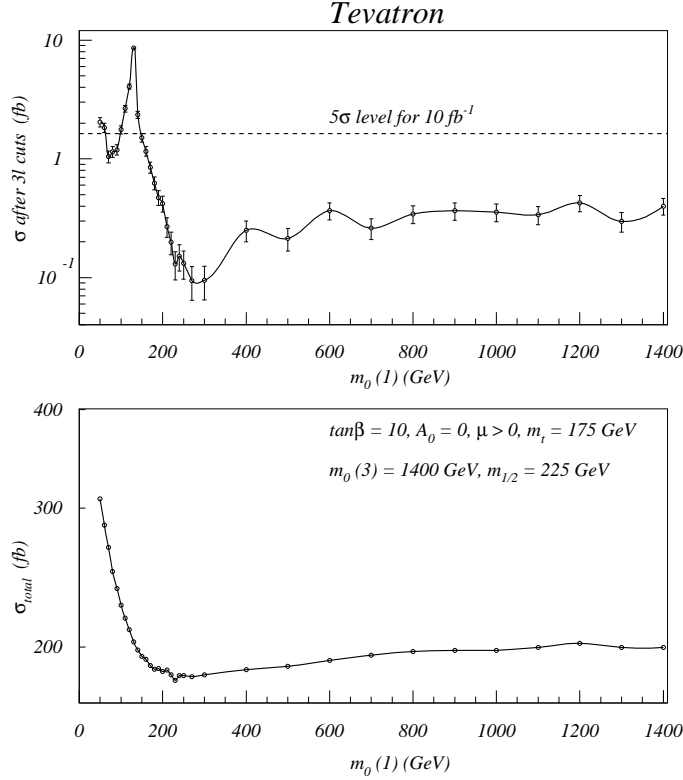


Figure 11: Rates for isolated trilepton events at the Fermilab Tevatron $p\bar{p}$ collider, after cuts SC2 from Ref. [43].

Tevatron doesn't always occur, even if $m_0(1)$ is small.

4.2 CERN LHC

The reach of the CERN LHC for SUSY particles in the mSUGRA model extends up to $m_{1/2}$ values as high as 1400 GeV (700 GeV) for small (large) values of the parameter m_0 , assuming 100 fb^{-1} of integrated luminosity[45]. This corresponds to a reach in $m_{\tilde{g}}$ of 3 (1.8) TeV, respectively. For the case of the NMH SUGRA model, $m_{1/2}$ is bounded from above by the requirement that the neutralino, and not a slepton, is the LSP. The upper bound on $m_{1/2}$ is well below the LHC reach in $m_{1/2}$ for the mSUGRA model, and so the CERN LHC should easily establish a signal in all of the NMH SUGRA model parameter space with low enough $m_0(1)$ values as to satisfy the $(g-2)_\mu$ deviation. A possible exception occurs if SUSY lies in the HB/FP region. But even here, first and second generation sleptons are relatively light, and may be accessible to LHC searches in the dilepton channel[46].

The collider signals for SUGRA-like models at the CERN LHC are naturally divided up according to number of leptons in the final state. Thus, in Ref. [45], signals for jets plus \cancel{E}_T plus 0, 1, 2 same sign (SS) or 2 opposite sign leptons (OS), 3 leptons and 4 or more leptons occur. In Fig. 12, we plot signal rates from the NMH SUGRA model for $m_0(3) = 2300 \text{ GeV}$, $m_{1/2} = 300 \text{ GeV}$, $A_0 = 0$, $\tan\beta = 10$ and $\mu > 0$, versus $m_0(1)$. The

cuts are listed in Ref. [45], and have been optimized to give best signal-to-background ratio for $m_0(1) = 100$ GeV. For very large $m_0(1) \simeq m_0(3)$ (mSUGRA model case), a variety of nonleptonic and multilepton signals occur, all at observable levels above background estimates. As $m_0(1)$ decreases, the total sparticle production cross section increases substantially, mainly because first and second generation squarks are decreasing in mass, and enhancing strongly interacting sparticle pair production rates. As $m_0(1)$ decreases further, leptonic rates also increase, in part because of increased total production cross sections, but also due to enhanced chargino and neutralino (s)leptonic branching fractions. As $m_0(1)$ drops below about 200 GeV (the value typically needed to explain the $(g-2)_\mu$ anomaly), multilepton rates rise steeply. Thus, we would expect that SUSY as manifested in the NMH SUGRA model would be easily discovered, and what's more, the signal events would be unusually rich in multilepton events. Such multilepton events can be especially useful for reconstructing sparticle masses in gluino and squark cascade decay events[47].

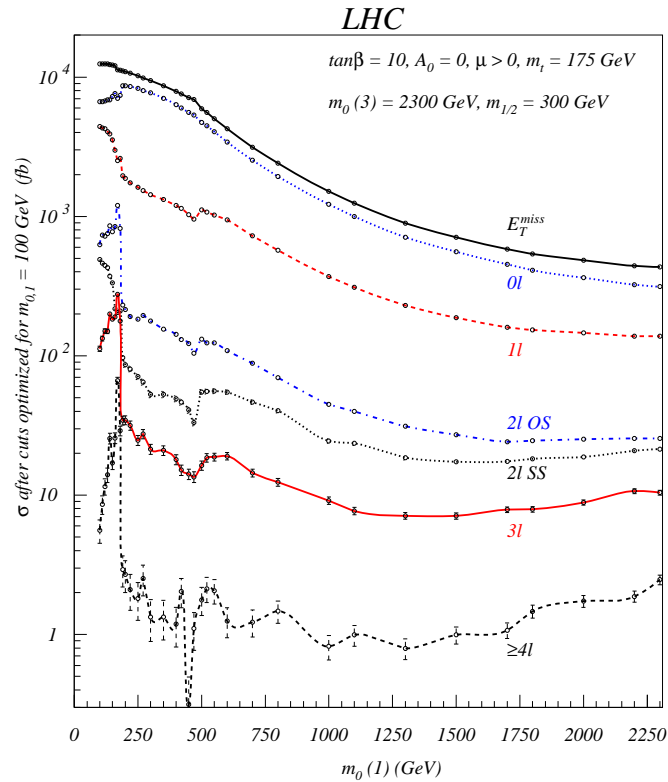


Figure 12: Rates for various SUSY signals at the CERN LHC, using cuts from Ref. [45]. The 5σ discovery cross section for the $\cancel{E}_T + \text{jets}$ channel for 100 fb^{-1} of integrated luminosity is 53.4 fb .

4.3 e^+e^- linear collider

A linear collider operating at $\sqrt{s} = 0.5 - 1 \text{ TeV}$ may be the next frontier particle physics accelerator beyond the CERN LHC. Depending on sparticle masses and the collider energy, charginos and neutralinos may or may not be accessible. However, in the NMH SUGRA

model, light first and second generation sleptons are needed both to explain the $(g - 2)_\mu$ anomaly, but also to enhance neutralino annihilation in the early universe. This means slepton masses are typically in the 100-300 GeV range, and likely within reach of a linear e^+e^- collider[48].

5. Conclusions

In this paper, we have examined the parameter space of gravity mediated SUSY breaking models, to see if constraints from $(g - 2)_\mu$, WMAP $\Omega_{\tilde{Z}_1} h^2$ and $BF(b \rightarrow s\gamma)$ can simultaneously be satisfied. In performing this task, we used new theoretical and experimental determinations of $(g - 2)_\mu$ which make use of $e^+e^- \rightarrow hadrons$ data at low energy to fix the hadronic vacuum polarization contribution to $a_\mu = (g - 2)_\mu$, and which gives a $\sim 3\sigma$ discrepancy with the SM. While $(g - 2)_\mu$ favors a spectrum of relatively light second generation sleptons, the $BF(b \rightarrow s\gamma)$ measurement favors relatively heavy (TeV scale) third generation squarks. Satisfying all constraints is possible in the mSUGRA model in only very limited regions: the stau co-annihilation region at low $\tan\beta \sim 10$, and in the A -annihilation funnel at very large $\tan\beta$. In particular, the HB/FP region gives only a tiny contribution to $(g - 2)_\mu$, and is disfavored by about 3σ if the e^+e^- data is used for the hadronic vacuum polarization determination.

We advocate relaxing the universality assumption between third generation scalars and their first and second generation counterparts. Simultaneously fulfilling all three constraints favors low values of $m_0(1) \simeq m_0(2) \sim 50 - 200$ GeV, while $m_0(3)$ values of a TeV or beyond are preferred. This comprises a normal scalar mass hierarchy, or NMH, at the GUT scale. The weak scale mass splittings amongst the squarks can be modest in NMH SUGRA scenario, even though mass splittings at M_{GUT} are large. The FCNC constraints from $B_d - \bar{B}_d$ and $BF(b \rightarrow s\gamma)$ are very weak and hardly affect the NMH SUGRA model parameter space. However, the weak scale splitting amongst sleptons is large, with selectrons and smuons in the 100 - 300 GeV range, while staus are in the TeV range. Neutralinos in the early universe annihilate via a combination of t -channel slepton exchange and slepton co-annihilation.

A testable consequence of the NMH scenario is that sleptons may be directly observable at the CERN LHC, provided that the slepton-neutralino mass gap isn't too small. In addition, the presence of relatively light sleptons enhances the rates for multilepton production in SUSY cascade decay events at the CERN LHC. The light sleptons might also lead to observable rates for trilepton events at the Fermilab Tevatron collider. Finally, selectrons, smuons and their associated sneutrinos in the 100 - 300 GeV mass range should be accessible to a linear e^+e^- collider operating at $\sqrt{s} = 0.5 - 1$ TeV, even if squarks and third generation sleptons are beyond the limit for direct searches.

Acknowledgments

We thank X. Tata for discussions. A.B. would like to thank David Hertzog for very useful and stimulating discussions at ASPEN03 conference. This research was supported in part

by the U.S. Department of Energy under contract number DE-FG02-97ER41022.

Appendix

In this appendix, we describe the “minimal mixing” scenario for soft SUSY breaking mass terms we adopted for our study, and apply it to constraints from $BF(b \rightarrow s\gamma)$ [5]. (Our notation is similar to that of [38].) The relevant Lagrangian terms are

$$\mathcal{L} \ni -\tilde{Q}_i^\dagger (\mathbf{m}_Q^2)_{ij} \tilde{Q}_j + \left((\mathbf{a}_d)_{ij} \tilde{Q}_i^a H_{da} \tilde{d}_{Rj}^\dagger + h.c. \right), \quad (5.1)$$

where $i, j = 1 - 3$ are generation indices and a is an $SU(2)$ index. We will ignore the possibility of large CP violating phases for this sample analysis.

Constraints are generally presented in terms of soft SUSY breaking matrix elements in the super-CKM basis, where quark mass matrices are diagonalized by

$$\mathbf{m}_u = v_u V_R^u \mathbf{f}_u^T V_L^{u\dagger} \quad \text{and} \quad \mathbf{m}_d = v_d V_R^d \mathbf{f}_d^T V_L^{d\dagger}, \quad (5.2)$$

and where the CKM matrix is given by $K \equiv V_L^u V_L^{d\dagger}$. We adopt a basis wherein \mathbf{f}_u is already diagonal, so that $V_L^{u\dagger} = V_R^u = \mathbf{1}$ and $K = V_L^{d\dagger}$.

At $Q = M_{GUT}$ the SSB mass-squared matrix has the form

$$\mathbf{m}_Q^2 = \begin{bmatrix} m_0^2(1) & 0 & 0 \\ 0 & m_0^2(1) & 0 \\ 0 & 0 & m_0^2(3) \end{bmatrix}, \quad (5.3)$$

while the trilinear matrix \mathbf{a}_d has only one non-zero entry given by $(\mathbf{a}_d)_{33} = f_b A_0$, where f_b is the b -quark Yukawa coupling.

In the minimal mixing scenario, the generation of off-diagonal terms in the running from M_{GUT} to M_{weak} is neglected. Therefore all off-diagonal elements in the down type squark mass matrix sub-blocks $(\mathbf{m}_d^2)_{LL}$ and $(\mathbf{m}_d^2)_{LR}$ arise from the rotation to the super-CKM basis. These off-diagonal elements are of the order $(\Delta_d)_{LL} \lesssim 10^{-2} \times (m_{d1}^2)_{LL}$ while $(\Delta_d)_{LR} \lesssim 10^{-4} \times (m_{d3}^2)_{LL}$. For example, for our sample parameter space point given by (3.4) these matrices will have the following numerical form

$$(\mathbf{m}_d^2)_{LL} \simeq \begin{bmatrix} 1.56 \times 10^6 & -39.3 & 2550 \\ -39.3 & 1.56 \times 10^6 & -1.8 \times 10^4 \\ 2550 & -1.8 \times 10^4 & 2.0 \times 10^6 \end{bmatrix}, \quad (5.4)$$

and

$$(\mathbf{m}_d^2)_{LR} \simeq \begin{bmatrix} -0.1 & 0.9 & -22.2 \\ 0.9 & -6.6 & 160.3 \\ -22.2 & 160.3 & -3909 \end{bmatrix}, \quad (5.5)$$

where all entries are in units of GeV^2 .

It is also possible to go a step further than the minimal mixing scenario and include (two-loop) RG evolution of SSB matrices \mathbf{m}_Q^2 and \mathbf{a}_d from $Q = M_{GUT}$ to $Q = M_Z$ to

generate flavor violating soft terms. We have checked using SoftSUSY[49] that these off-diagonal elements would be of the same order of magnitude as off-diagonal elements of SSB matrices in the minimal mixing scenario after rotation to super-CKM basis. Therefore, for our order-of-magnitude estimation the minimal mixing scenario appears justified. For example, for our sample parameter space point (3.4), the SSB matrices after RG running from M_{GUT} to M_Z will have the following numerical form:

$$\mathbf{m}_Q^2 \simeq \begin{bmatrix} 1.56 \times 10^6 & -43 & -660 \\ -43 & 1.56 \times 10^6 & -7625 \\ -660 & -7626 & 2.0 \times 10^6 \end{bmatrix} \quad (5.6)$$

(units of GeV^2), and

$$\mathbf{a}_d \simeq \begin{bmatrix} -2.1 & -4.1 & -2.3 \\ -4.1 & -20.0 & -28.1 \\ -2.2 & -25.9 & -665.1 \end{bmatrix} \quad (5.7)$$

(in units of GeV).

A rotation of the down squark sub-block mass matrices to the super-CKM basis yields

$$(\mathbf{m}_d^2)_{LL} \simeq \begin{bmatrix} 1.56 \times 10^6 & -164 & 3601 \\ -164 & 1.56 \times 10^6 & -2.6 \times 10^4 \\ 3601 & -2.6 \times 10^4 & 2.0 \times 10^6 \end{bmatrix}, \quad (5.8)$$

and

$$(\mathbf{m}_d^2)_{LR} \simeq \begin{bmatrix} -6.7 & 0.04 & 1.1 \\ 0.04 & -116.4 & -8.4 \\ -0.66 & 4.2 & -3922.8 \end{bmatrix}. \quad (5.9)$$

In this example at least, it is clear that the off-diagonal elements after including RG evolution are of the same order of magnitude as those in the minimal mixing scenario.

One should also notice that $(\Delta_d)_{LL}$ is proportional to $m_{d3}^2 - m_{d1}^2$, which in our scenario is of the order $(\text{TeV})^2$, while the $(\Delta_d)_{LR}$ elements are at most of the order $(10 \text{ GeV})^2$ and therefore contributions from A terms can be neglected in our estimates of constraints from Δm_K and Δm_B .

The general bounds from $BF(b \rightarrow s\gamma)$ on these matrix elements from [5] are :

$$(\Delta_d^{23})_{LL} < 8.2 \left(\frac{m_{\tilde{q}}}{500 \text{ GeV}} \right)^2 m_{\tilde{q}}^2 \quad (5.10)$$

which for $(\Delta_d^{23})_{LL} \sim 10^{-2} \times m_{\tilde{q}}^2$ implies $m_{\tilde{q}} > 17.5 \text{ GeV}$, which is easily satisfied. Also,

$$(\Delta_d^{23})_{LR} < 0.016 \left(\frac{m_{\tilde{q}}}{500 \text{ GeV}} \right)^2 m_{\tilde{q}}^2 \sim 64 \text{ GeV}^2 \quad (5.11)$$

for $m_{\tilde{q}} \sim 1 \text{ TeV}$. Thus, the assumed mass splittings in the NMH scenario seem safe from FCNC constraints when minimal mixing is assumed.

References

- [1] A. Chamseddine, R. Arnowitt and P. Nath, *Phys. Rev. Lett.* **49** (1982) 970; R. Barbieri, S. Ferrara and C. Savoy, *Phys. Lett.* **B 119** (1982) 343; N. Ohta, *Prog. Theor. Phys.* **70** (1983) 542; L. J. Hall, J. Lykken and S. Weinberg, *Phys. Rev.* **D 27** (1983) 2359; for reviews, see H. P. Nilles, *Phys. Rept.* **110** (1984) 1 and P. Nath, [hep-ph/0307123](#).
- [2] E. Cremmer, S. Ferrara, L. Girardello and A. van Proeyen, *Nucl. Phys.* **B 212** (1983) 413.
- [3] S. Dimopoulos and H. Georgi, *Nucl. Phys.* **B 193** (1981) 150.
- [4] S. K. Soni and H. A. Weldon, *Phys. Lett.* **B 126** (1983) 215; V. Kaplunovsky and J. Louis, *Phys. Lett.* **B 306** (1993) 269
- [5] F. Gabbiani, E. Gabrielli, A. Masiero and L. Silvestrini, *Nucl. Phys.* **B 477** (1996) 321.
- [6] A. Masiero and L. Silvestrini, [hep-ph/9711401](#).
- [7] K. Choi, J. S. Lee and C. Munoz, *Phys. Rev. Lett.* **80** (1998) 3686.
- [8] H. Baer, C. Balazs, A. Belyaev, J. Mizukoshi, X. Tata and Y. Wang, *J. High Energy Phys.* **0207** (2002) 050 and [hep-ph/0210441](#); for a review, see G. Eigen, R. Gaitskell, G. Kribs and K. Matchev, [hep-ph/0112312](#).
- [9] K. Abe *et al.* (Belle Collaboration), *Phys. Lett.* **B 511** (2001) 151.
- [10] D. Cronin-Hennessy *et al.* (Cleo Collaboration), *Phys. Rev. Lett.* **87** (2001) 251808.
- [11] R. Barate *et al.* (Aleph Collaboration), *Phys. Lett.* **B 429** (1998) 169.
- [12] P. Gambino and M. Misiak, *Nucl. Phys.* **B 611** (2001) 338.
- [13] Theoretical results for $BF(b \rightarrow s\gamma)$ in the SM are contained in *e.g.* P. Gambino and M. Misiak, *Nucl. Phys.* **B 611** (2001) 338.
- [14] We use the supersymmetric calculation of $BF(b \rightarrow s\gamma)$ as presented in H. Baer and M. Brhlik, *Phys. Rev.* **D 55** (1997) 3201 and H. Baer, M. Brhlik, D. Castano and X. Tata, *Phys. Rev.* **D 58** (1998) 015007.
- [15] G. Bennett *et al.* (E821 Collaboration), *Phys. Rev. Lett.* **89** (2002) 101804 and [hep-ex/0401008](#) (2004).
- [16] M. Davier, S. Eidelman, A. Hocker and Z. Zhang, *Eur. Phys. J.* **C 31** (2003) 503.
- [17] K. Hagiwara, A. D. Martin, D. Nomura and T. Teubner, [hep-ph/0312250](#) (2003).
- [18] J. Feng and K. Matchev, *Phys. Rev. Lett.* **86** (2001) 3480; we use the calculation of H. Baer, C. Balazs, J. Ferrandis and X. Tata, *Phys. Rev.* **D 64** (2001) 035004, which is based upon expressions in T. Moroi, *Phys. Rev.* **D 53** (1996) 6565.
- [19] D. N. Spergel *et al.*, Determination of Cosmological Parameters,” *Astrophys. J.* **148** (2003) 175.
- [20] For recent reviews, see *e.g.* W. Freedman and M. Turner, *Rev. Mod. Phys.* **75** (2003) 1433; A. Lahanas, N. Mavromatos and D. Nanopoulos, *Int. J. Mod. Phys.* **D 12** (2003) 1529.
- [21] J. Ellis, T. Falk and K. Olive, *Phys. Lett.* **B 444** (1998) 367; J. Ellis, T. Falk, K. Olive and M. Srednicki, *Astropart. Phys.* **13** (2000) 181.

- [22] K. Chan, U. Chattopadhyay and P. Nath, *Phys. Rev. D* **58** (1998) 096004; J. Feng, K. Matchev and T. Moroi, *Phys. Rev. Lett.* **84** (2000) 2322 and *Phys. Rev. D* **61** (2000) 075005; J. Feng, K. Matchev and F. Wilczek, *Phys. Lett. B* **482** (2000) 388 and *Phys. Rev. D* **63** (2001) 045024; the HB/FP region also appears in H. Baer, C. H. Chen, F. Paige and X. Tata, Ref. [45] and in H. Baer, C. H. Chen, C. Kao and X. Tata, *Phys. Rev. D* **52** (1995) 1565.
- [23] M. Drees and M. Nojiri, *Phys. Rev. D* **47** (1993) 376; H. Baer and M. Brhlik, *Phys. Rev. D* **57** (1998) 567; H. Baer, M. Brhlik, M. Diaz, J. Ferrandis, P. Mercadante, P. Quintana and X. Tata, *Phys. Rev. D* **63** (2001) 015007; A. Djouadi, M. Drees and J. Kneur, *J. High Energy Phys.* **0108** (2001) 055; J. Ellis, T. Falk, G. Ganis, K. Olive and M. Srednicki, *Phys. Lett. B* **510** (2001) 236; L. Roszkowski, R. Ruiz de Austri and T. Nihei, *J. High Energy Phys.* **0108** (2001) 024; A. Lahanas and V. Spanos, *Eur. Phys. J. C* **23** (2002) 185.
- [24] H. Baer and C. Balazs, *JCAP* **0305** (2003) 006.
- [25] S. Narison, *Phys. Lett. B* **568** (2003) 231.
- [26] J. Feng, C. Kolda and N. Polonsky, *Nucl. Phys. B* **546** (1999) 3; J. Bagger, J. Feng and N. Polonsky, *Nucl. Phys. B* **563** (1999) 3; J. Bagger, J. Feng, N. Polonsky and R. Zhang, *Phys. Lett. B* **473** (2000) 264; H. Baer, P. Mercadante and X. Tata, *Phys. Lett. B* **475** (2000) 289; H. Baer, C. Balazs, P. Mercadante, X. Tata and Y. Wang, *Phys. Rev. D* **63** (2001) 015011; H. Baer, C. Balazs, M. Brhlik, P. Mercadante, X. Tata and Y. Wang, *Phys. Rev. D* **64** (2001) 015002.
- [27] F. Paige, S. Protopopescu, H. Baer and X. Tata, hep-ph/0312045.
- [28] B. Allanach, S. Kraml and W. Porod, *J. High Energy Phys.* **0303** (2003) 016; for recent results, see the website <http://kraml.home.cern.ch/kraml/comparison/compare.html>.
- [29] P. Gondolo and G. Gelmini, *Nucl. Phys. B* **360** (1991) 145; J. Edsjo and P. Gondolo, *Phys. Rev. D* **56** (1997) 1879
- [30] H. Baer, C. Balazs and A. Belyaev, *J. High Energy Phys.* **0203** (2002) 042 and hep-ph/0211213; this is based on earlier work by H. Baer and M. Brhlik, *Phys. Rev. D* **52** (1995) 5031.
- [31] H. Anlauf, *Nucl. Phys. B* **430** (1994) 245.
- [32] M. Ciuchini, E. Franco, G. Martinelli and L. Reina, *Nucl. Phys. B* **415** (1994) 403; M. Misiak and M. Münz, *Phys. Lett. B* **344** (1995) 308.
- [33] C. Greub, T. Hurth and D. Wyler, *Phys. Lett. B* **380** (1996) 385 and *Phys. Rev. D* **54** (1996) 3350.
- [34] M. Carena, D. Garcia, U. Nierste and C. Wagner, *Phys. Lett. B* **499** (2001) 141.
- [35] G. Degrossi, P. Gambino and G. Giudice, *J. High Energy Phys.* **0012** (2000) 009.
- [36] H. Baer, M. Diaz, P. Quintana and X. Tata, *J. High Energy Phys.* **0004** (2000) 016.
- [37] J. Hagelin, S. Kelley and T. Tanaka, *Nucl. Phys. B* **415** (1994) 293.
- [38] M. Misiak, S. Pokorski and J. Rosiek, *Adv. Ser. Direct. High Energy Phys.* **15**, 795 (1998).
- [39] H. Baer, B. Harris and M. H. Reno, *Phys. Rev. D* **57** (1998) 5871.
- [40] H. Baer, C. H. Chen, F. Paige and X. Tata, *Phys. Rev. D* **49** (1994) 3283.

- [41] H. Baer, C. H. Chen, C. Kao and X. Tata, *Phys. Rev. D* **52** (1995) 1565; H. Baer, C. H. Chen, F. Paige and X. Tata, *Phys. Rev. D* **54** (1996) 5866; H. Baer, C. H. Chen, M. Drees, F. Paige and X. Tata, *Phys. Rev. D* **58** (1998) 075008.
- [42] H. Baer, K. Hagiwara and X. Tata, *Phys. Rev. Lett.* **57** (1986) 294 and *Phys. Rev. D* **35** (1987) 1598; P. Nath and R. Arnowitt, *Mod. Phys. Lett. A* **2** (1987) 331; R. Barbieri, F. Caravaglios, M. Frigeni and M. Mangano, *Nucl. Phys. B* **367** (1991) 28; H. Baer and X. Tata, *Phys. Rev. D* **47** (1993) 2739; H. Baer, C. Kao and X. Tata, *Phys. Rev. D* **48** (1993) 5175.
- [43] H. Baer, T. Krupovnickas and X. Tata, *J. High Energy Phys.* **0307** (2003) 020; see also H. Baer, M. Drees, F. Paige, P. Quintana and X. Tata, *Phys. Rev. D* **61** (2000) 095007; V. Barger and C. Kao, *Phys. Rev. D* **60** (1999) 115015; K. Matchev and D. Pierce, *Phys. Lett. B* **467** (1999) 225 for earlier work on the trilepton signal.
- [44] See H. Baer, M. Drees, F. Paige, P. Quintana and X. Tata, Ref. [43].
- [45] H. Baer, C. Balazs, A. Belyaev, T. Krupovnickas and X. Tata, *J. High Energy Phys.* **0306** (2003) 054. For earlier work, see H. Baer, C. H. Chen, F. Paige and X. Tata, *Phys. Rev. D* **52** (1995) 2746 and *Phys. Rev. D* **53** (1996) 6241; H. Baer, C. H. Chen, M. Drees, F. Paige and X. Tata, *Phys. Rev. D* **59** (1999) 055014; S. Abdullin and F. Charles, *Nucl. Phys. B* **547** (1999) 60; S. Abdullin *et al.* (CMS Collaboration), [hep-ph/9806366](#); B. Allanach, J. Hetherington, A. Parker and B. Webber, *J. High Energy Phys.* **08** (2000) 017.
- [46] See H. Baer *et al.*, Ref. [40]; see also D. Denegri, W. Majerotto and L. Rurua, *Phys. Rev. D* **58** (1998) 095010; Y. Andreev, S. Bitjukov and N. Krasnikov, [hep-ph/0402229](#).
- [47] I. Hinchliffe, F. Paige, M. Shapiro, J. Soderqvist and W. Yao, *Phys. Rev. D* **55** (1997) 5520.
- [48] H. Baer, A. Belyaev, T. Krupovnickas and X. Tata, *J. High Energy Phys.* **0402** (2004) 007.
- [49] B. Allanach, *Comput. Phys. Commun.* **143** (2002) 305.